ACS OMEGA

http://pubs.acs.org/journal/acsodf

Article

High-Yield and High-Efficiency Conversion of HMF to Levulinic Acid in a Green and Facile Catalytic Process by a Dual-Function Brønsted-Lewis Acid $HScCl_4$ Catalyst

Shiwei Liu, Xueli Cheng, Shiqin Sun, Yige Chen, Bing Bian, Yue Liu,* Li Tong, Hailong Yu,* Yonghao Ni, and Shitao Yu

Cite This: *ACS Omega* 2021, 6, 15940−15947

Read Online

ACCESS | Metrics & More | Article Recommendations | Supporting Information

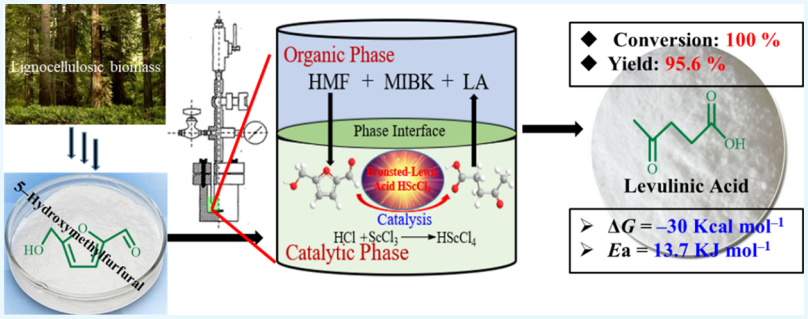

ABSTRACT: Lignocellulosic biorefineries have received considerable attention for the purpose of producing high-value chemicals and materials. Levulinic acid (LA) is an important biomass-derived platform chemical that is produced from sugar-based biomass. Unfortunately, the catalysts reported thus far have shortcomings, such as expensive starting materials, complicated synthesis or purification operations, and a low LA yield under harsh reaction conditions. Herein, we develop a novel dual-functional catalyst, $HScCl_4$, by combining Brønsted acid (HCl) and Lewis acid ($ScCl_3$) sites. The as-prepared $HScCl_4$ catalyst shows high efficiency and high selectivity for converting 5-hydroxymethylfurfural (HMF) to LA in a biphasic system consisting of methyl isobutyl ketone (MIBK) and water. The density functional theory (DFT) results show that the synergistic catalytic effect, originating from the Brønsted and Lewis acidic sites of $HScCl_4$, significantly decreases the energy barriers of reactants and intermediates, thus facilitating the conversion of HMF to LA. Moreover, the efficient separation of LA in the water-MIBK biphasic system by extracting LA to the MIBK phase minimizes the side reactions of LA and thus the formation of humins while significantly improving the LA yield. The conversion of HMF and the selectivity for LA are 100 and 95.6% at 120 °C for 35 min, respectively. The free energy (ΔG) and activation energy (E_a) of the reaction are −30 kcal mol^{-1} and 13.7 kJ mol^{-1}, respectively. The developed process provides a green, sustainable, and efficient pathway to produce LA from biomass-derived HMF under mild conditions.

1. INTRODUCTION

Lignocellulosic biomass, one of the most abundant renewable resources, has been regarded as an attractive renewable carbon source for biofuels and bio-based platform chemicals.[1] Particularly, as one of the three major components of lignocellulosic biomass, cellulose is a macromolecular polymer existing in nature that has become a valuable raw material for the production of chemical and biomedical materials.[2−4] The effective conversion to platform chemicals such as levulinic acid (LA) has attracted much attention.[5] However, due to the water-insoluble characteristics and the robust structure of cellulose, the reaction of the conversion of cellulose to LA usually needs harsh reaction conditions, and the LA yield is low. Various studies on the synthesis of LA from cellulose, glucose, and fructose have been performed,[6−8] and different catalysts, including solid acids,[9,10] inorganic acids,[11] and ionic liquids (ILs),[12−14] have been investigated. However, these catalysts studied thus far suffer shortcomings, such as expensive starting materials, harsh experimental conditions, and complicated synthesis and purification operations. Some studies have been performed on the synthesis of LA from 5-hydroxymethylfurfural (HMF) and different catalysts (Table 1), including inorganic acids (H_2SO_4, HCl),[15,16] solid catalysts (Fe/Hβ-zeolite),[17] and ILs ([IL-SO_3H]Cl + $NiSO_4$).[4,14,18] Although some catalysts can achieve a high yield of LA,

Received: March 25, 2021
Accepted: May 26, 2021
Published: June 9, 2021

Table 1. Comparison of Reaction Conditions and Results of the Present Study with Those Reported in the Literature

catalyst	T/°C	t/min	conversion/%	yield/%	E_a/kJ mol^{-1}	references
H_2SO_4	141	12	100	85.3	110	15
HCl	270	3.3	100	76.5	94.1	16
HCl	180	240	86.5	42.4	92	8
H_3PO_4 + $CrCl_3$	170	120	100	69.0	60.6	19
Fe/Hβ-zeolite	160	240	100	87.6	61	17
[IL-SO_3H]Cl + $NiSO_4$	175	120	100	56.3	34.3	14
β-zeolite + HCl	135	480	82.2	61.7	33	20
$HScCl_4$	120	35	100	95.6	13.7	this work

disadvantages such as complicated synthesis, corrosion equipment, and difficulty in separation and purification exist. Compared to Brønsted or Lewis acid catalysts and other catalysts, the concept of using both Brønsted and Lewis acids in the same system improves catalytic performance for the conversion of HMF to LA.[4,18]

To date, the LA yield results reported in the literature are usually low due to the side reactions occurring in the reaction system, which is typically a single-phase (water) system, where the condensations or polymerizations of reactants/intermediates/products occur, leading to the formation of humins.[8,14] Recent studies have shown that the biphasic reaction system, whereby the reactant and product are present in different phases, is of interest for high-yield conversion of biomass to the desirable product (including HMF to LA) due to the minimization of side reactions. Thus, the biphasic system is regarded as a promising process technology for biomass conversion to high-value chemicals.[18,21]

Rare earth metal-based Lewis acid catalysts have been shown to have excellent catalytic performance for reactions such as polyaddition,[22] hydration,[23] and polymerization.[24] Compared to d-series transition metals (such as Cr, Ti, and Fe), the rare earth metal possesses an abundant number of coordination sites. For example, the coordination number of Sc can reach up to 9−12,[25] which can effectively coordinate with heteroatoms, such as O, N, and S. The high coordination numbers can help facilitate high reactivity and selectivity in many reactions.[24]

In this study, we developed a novel dual-function acid catalyst, $HScCl_4$, by combining rare earth metal-based Lewis acid-$ScCl_3$ and Brønsted acid-HCl. It was then applied to catalyze the conversion of HMF to LA in a biphasic system consisting of methyl isobutyl ketone (MIBK) and water. The $HScCl_4$ catalyst shows highly efficient and highly selective conversion of HMF to LA. The synergistic catalytic effect, originating from the Brønsted and Lewis acidic sites of $HScCl_4$, obviously decreases the energy barriers of reactants and intermediates, which facilitates the conversion of HMF to LA. Moreover, the efficient separation of the water−MIBK biphasic system by extracting LA to the MIBK phase could minimize the side reactions of LA and significantly improve the yield of LA. Thus, the formation of humins decreased.

2. RESULTS AND DISCUSSION

2.1. Analysis of the Frontier Molecular Orbital for Conversion HMF to LA. We proposed a possible mechanism for the conversion of HMF to LA using the dual-function Brønsted−Lewis acid $HScCl_4$ catalyst (Figure 1a) based on available information in the literature.[26−28] This process involves five steps: C═C bond hydration of HMF to form intermediate IC1 (step 1), dehydration of IC1 to generate intermediate IC2 (step 2), which are consistent with the previous findings of Li et al.,[28] C−O bond cleavage of IC2 to produce intermediate IC3 with the 1,2-dicarbonyl structure (step 3), which has been reported by Velaga et al.,[27] decarboxylation of IC3 to produce intermediate IC4 and formic acid (step 4), and hydration-negative hydrogen-transfer reaction of IC4 to form LA (step 5); the last two steps agree with the findings of Shi et al.[26]

Full structure analyses of the reactant (HMF), intermediates (IC1−IC4), transition states (TS1−TS5), and product (LA) in the absence or presence of catalysts were performed via the density functional theory (DFT) method to assess their highest occupied molecular orbital (HOMO) and lowest unoccupied molecular orbital (LUMO) energy levels and both energy gaps Δ|LUMO−HOMO| (Figures 1b and S1−S3, Table S1). As shown in Figure 1b, among all catalysts, the energy gap Δ|LUMO−HOMO| for HMF using the $HScCl_4$ catalyst is the lowest (3.15 eV), which is 1.88 and 0.01 eV lower than those of the HCl and $ScCl_3$ catalysts, respectively. Additionally, the optimized structure of HMF + $HScCl_4$ shows that the coordination (Sc^{3+} ← O) of the Lewis acid site Sc^{3+} with O (C−O−C) and the protonation (H^+ ← C═C) of Brønsted acid site H^+ with a C═C bond occur simultaneously (Figure S1, HMF + $HScCl_4$).

When either HCl or $ScCl_3$ is used alone, only one coordination (Sc^{3+} ← O) or protonation (H^+ ← C═C) is possible (Figure S1, HMF + HCl and HMF + $ScCl_3$), which is consistent with observations in the literature.[4,29] Compared with the single coordination or protonation of the catalyst HCl or $ScCl_3$, the combined actions of the dual-function $HScCl_4$ catalyst produce a synergistic inductive effect on HMF, significantly improving the ^{2}C positive charge of the furan ring (Figure S1, HMF + $HScCl_4$), thus facilitating the hydration of C═C of HMF to transition state TS1, which agrees with that in the literature (Figure 1a, step 1).[30] Therefore, the dual-function $HScCl_4$ catalyst has excellent activation of HMF. Furthermore, the $HScCl_4$ catalyst also significantly decreases the energy gaps Δ|LUMO−HOMO| of intermediates IC1−IC4 (Figure 1b), thus facilitating the conversion of HMF to LA.

We also calculated the orbital energy levels and energy gaps of transition states TS1−TS5 in the presence of the dual-function $HScCl_4$ catalyst (Figure 1c). Based on our DFT results and those in the literature,[31,32] all the energy gaps Δ|LUMO−HOMO| of transition states TS1−TS5 are less than 6.0 eV, indicating that they are activated by the $HScCl_4$ catalyst. Additionally, all transition states have only one imaginary frequency, and their energies at 0 K are the highest energy point, indicating that the structures of the transition states are credible (Table S1, Figures S4−S8). Therefore, the dual-function $HScCl_4$ catalyst has thermodynamically favorable transition states, which is beneficial to lowering the activation

https://doi.org/10.1021/acsomega.1c01607
ACS Omega 2021, 6, 15940−15947

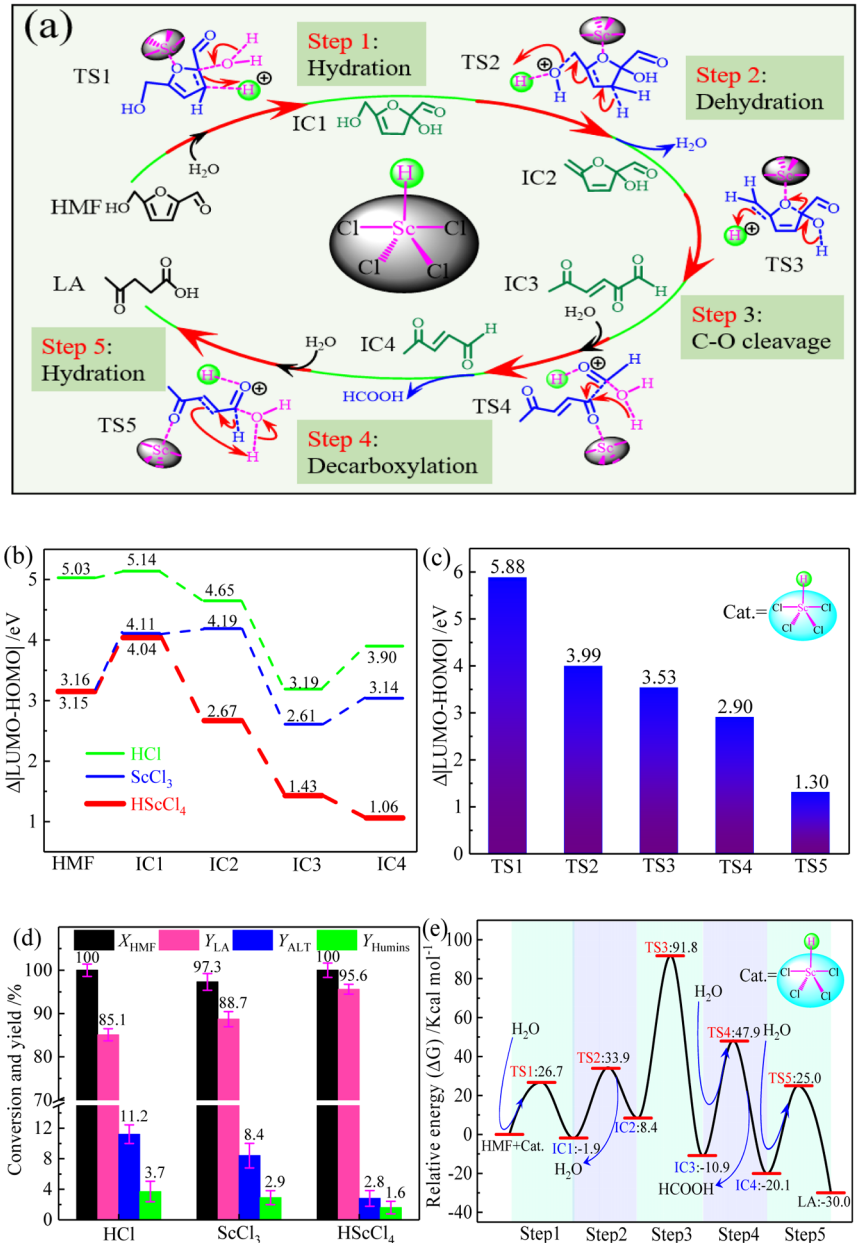

Figure 1. (a) Proposed mechanism for the conversion of HMF to LA in the presence of the $HScCl_4$ catalyst. (b) Orbital energy gaps Δ|LUMO−HOMO| of HMF and intermediates IC1−IC4 over different catalysts. (c) Orbital energy gaps Δ|LUMO−HOMO| of transition states TS1−TS5 over the $HScCl_4$ catalyst. (d) Effects of the different catalysts on the conversion of HMF and yields for various products [reaction conditions: 1.0 g of HMF, 10 mL of MIBK, and 0.27 mmol of the catalyst $HScCl_4$ (in situ synthesized by 0.27 mmol of $ScCl_3$ and 3.0 g of 0.33 wt % HCl), T = 120 °C, t = 35 min]. (e) Relative free-energy (ΔG) profile in the presence of the $HScCl_4$ catalyst.

energy, thus favoring the conversion of HMF to the desired product LA.

2.2. Effect of Different Catalysts for the Selective Conversion of HMF to LA. FTIR spectra using pyridine as a probe were used to study the types of acid sites of the bifunctional catalyst $HScCl_4$, and the results showed that three bands were observed (1442, 1489, and 1545 cm^{-1}), which were attributed to pyridine adsorbed on Lewis acid sites, a combination of Lewis and Brønsted acid sites, and pyridine interacting with Brønsted acid sites, respectively (Table S2, Figure S9). As shown in Figure 1d, the LA yield is significantly affected by the catalysts used. In the presence of the Brønsted acid HCl catalyst, the LA yield is the lowest (85.1%), with the formation of 3.7% humins and 11.2% angelica-lactone (ALT). In the presence of the Lewis acid $ScCl_3$ catalyst, the LA yield was 88.7%, with the formation of 2.9% humins and 8.4% ALT. In contrast, when the Brønsted−Lewis acid $HScCl_4$ catalyst is used, the yield for LA is the highest (95.6%), with the formation of only 1.6% humins and 2.8% ALT, much lower than those using HCl or $ScCl_3$ alone as the catalyst. Therefore, the order of the catalytic performance for conversion of HMF to LA is as follows: $HScCl_4$ > $ScCl_3$ > HCl, agreeing with those of DFT analyses (Figure 1c). These results support the conclusion that the dual-function $HScCl_4$ catalyst has excellent catalytic performance for HMF conversion to LA due to the synergistic catalytic effect originating from its double-acid sites.

Additionally, when formic acid was removed by distillation from the catalytic phase, the $HScCl_4$ catalyst was recovered

https://doi.org/10.1021/acsomega.1c01607
ACS Omega 2021, 6, 15940−15947

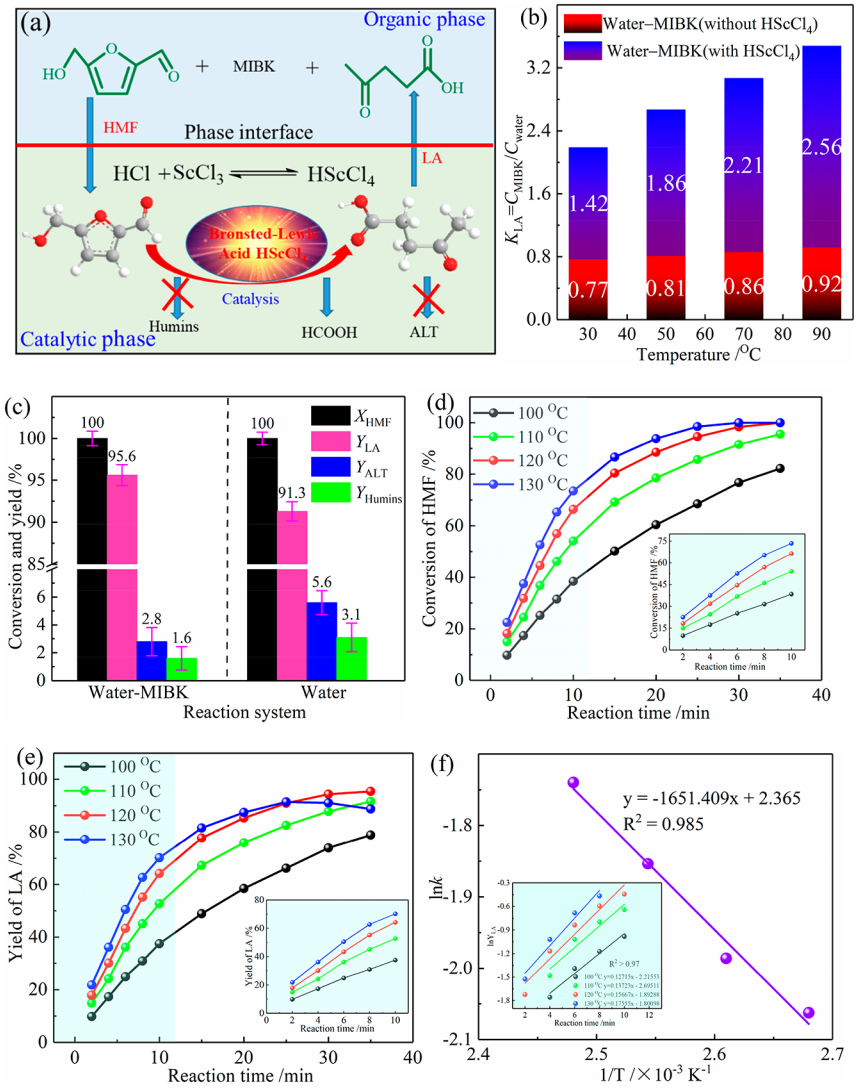

Figure 2. (a) Schematic diagram of the water−MIBK biphasic system. (b) Distribution coefficient of LA (K_{LA}) in a water−MIBK biphasic system as a function of temperature (conditions: 10.0 mL of MIBK, 1.0 g of LA, 3.0 mL of water, or 3.0 g of 0.33 wt % HCl aqueous solution with 0.27 mmol of $ScCl_3$). (c) Effects of the reaction system on the conversion of HMF to LA (reaction conditions: 1.0 g of HMF, 10 mL of MIBK, and 0.27 mmol of the catalyst $HScCl_4$ in situ synthesized by 0.27 mmol of $ScCl_3$ and 3.0 g of 0.33 wt % HCl, T = 120 °C, t = 35 min). (d,e) Effect of reaction temperature and time on the catalytic conversion of HMF and LA yield in the presence of the $HScCl_4$ catalyst. (f) Arrhenius graphs for the catalytic conversion of HMF to LA in the presence of the $HScCl_4$ catalyst.

and reused for the next time (Figure S10). The $HScCl_4$ catalyst was reused seven times without any obvious decrease in reaction conversion and product yields (X_{HMF} = 100%, Y_{LA} = 95.1%). Therefore, the $HScCl_4$ catalyst shows excellent reusable performance in the reaction. The good reusability of the $HScCl_4$ catalyst is attributed to its excellent thermal stability (Figure S12), which comes from the strong complex ability of Sc^{3+} with Cl^-.

2.3. Free Energy for HMF Conversion to LA. The free-energy (ΔG) profile for HMF conversion to LA in the presence of the dual-function $HScCl_4$ catalyst is shown in Figure 1e: (1) the formation of transition state TS1 from HMF by the dual-function $HScCl_4$ catalyst has a 26.7 kcal mol^{-1} energy barrier, while intermediate IC1 via the hydration reaction has an overall energy barrier of −1.9 kcal mol^{-1} (Figure 1a,e, step 1). (2) The 5-hydroxyl group of intermediate IC1 is activated by the Brønsted acid site (H^+), and simultaneously, the oxygen atom of the furan ring is activated from the coordination of the Lewis acid site (Sc^{3+}). Subsequently, dehydration and intramolecular C═C transfer lead to the formation of intermediate IC2, with a 10.3 kcal mol^{-1} energy barrier (Figure 1a,e, step 2). (3) The ether cleavage of intermediate IC2 forms intermediate IC3 through transition state TS3, and the critical driving force required is provided by the $HScCl_4$ catalyst. The energy barrier of 83.4 kcal mol^{-1} for TS3 is the highest among all transition states due to the high stability of the dihydrofuran ring, which is similar to the finding of Su et al. in the ring-opening reaction (Figure 1a,e, step 3).[33] (4) Intermediate IC3 is hydrated to form transition state TS4 with a 58.8 kcal mol^{-1} energy barrier, following the decarboxylation of IC3, yielding intermediate IC4 and formic acid (Figure 1a,e, step 4). (5) Intermediate IC4 is attacked by water to form transition state TS5, with a 45.1 kcal mol^{-1} energy barrier, followed by migration of a hydride, ultimately forming LA, with a 55.0 kcal mol^{-1} energy

https://doi.org/10.1021/acsomega.1c01607
ACS Omega 2021, 6, 15940−15947

release, where again, the critical driving force is provided by the $HScCl_4$ catalyst (Figure 1a,e, step 5).

For the overall reaction process, the highest energy barrier is the ether cleavage of intermediate IC2 (83.4 kcal mol^{-1}). Additionally, a total of 30 kcal mol^{-1} apparent energy is released for the HMF conversion to LA in the presence of the dual-function $HScCl_4$ catalyst. Yang et al. used the Bronsted acid site H^+ as a catalyst for the conversion of HMF to LA, and via DFT calculations, they found that the lowest free energy was −32.7 kcal mol^{-1} in the three reaction pathways.[34]

2.4. Effect of the Biphasic Reaction System for Selective Conversion of HMF to LA. The advantage of the water−MIBK biphasic system is shown in Figure 2c, where the conversion of HMF to LA is performed in water (without MIBK) under otherwise the same conditions. HMF is completely consumed, but the LA yield is 91.3% (in contrast to the 95.6% LA yield in the biphasic system), with the formation of 3.1% humins and 5.6% ALT (both are higher than those in the biphasic system at 1.6% and 2.8%, respectively). These results indicate that the efficient separation of LA in the water−MIBK biphasic system by extracting LA to the MIBK phase (Figure 2a) minimizes the side reactions of LA, thus leading to the increased LA yield. A similar advantage of the biphasic system, that is, increasing the product yield and minimizing the side reactions, was also reported in other reactions, such as asymmetric sulfoxidation, aldol reaction, and ammonia synthesis.[35−37]

The effective extraction of LA in the biphasic system is supported by the high distribution coefficient of LA (K_{LA}) in the water−MIBK biphasic system (Figure 2b), which is enhanced by the salt effect of $HScCl_4$.

2.5. Effect of Reaction Time and Temperature for Selective Conversion of HMF to LA. As shown in Figure 2d, the reaction temperature and time have significant effects on the conversion of HMF. The conversion of HMF obviously increases with increasing reaction temperature and time. The HMF conversion is only 82.2% at 100 °C for 35 min (Figure 2d), while it reaches 100% at 130 °C for 30 min.

The effects of different reaction temperatures and times on the LA yield are shown in Figure 2e. The highest LA yield increases from 78.8 to 95.6% as the temperature increases from 110 to 120 °C. At 130 °C, the LA yield reaches a maximum (92.3%) at 25 min and then sharply decreases to 88.7% at 35 min, which is due to the condensation/polymerization of HMF, the intermediates, and the conversion of LA to ALT. Similar side reactions were reported by Patil and Lund and Galletti et al. in the conversion of HMF and giant reed to LA, respectively.[38,39]

2.6. Kinetic Study on Selective Conversion of HMF to LA. The results used in this section were obtained within 10 min because during this period, the side reactions (condensations/polymerizations) were minimized. The kinetics at different temperatures is analyzed (Figures S13−S16). The activation energy (E_a), calculated from the slope of the Arrhenius plot, is 13.7 kJ mol^{-1} (Figure 2f), which is lower than the values reported in the literature (Figure 3),[8,14−17,19,20] supporting the advantages of the dual-function $HScCl_4$ catalyst. Notably, the catalyst can accelerate the reaction by stabilizing the transition states and decreasing the energy barriers. Furthermore, the obtained LA yield is very high (reaching 95.6%), even higher than the highest value reported in the literature (87.6%) at 160 °C for 240 min in the presence of Fe/Hβ-zeolite (Figure 3 and Table 1).[17] Kumar et al. reported

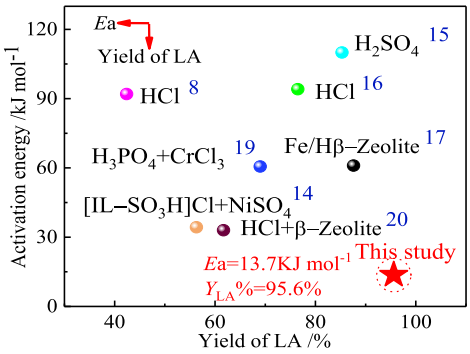

Figure 3. Comparison of the activation energy and LA yield for the catalytic conversion of HMF to LA of the present study with those reported in the literature.

that the reaction activation energy (E_a) is 34.3 kJ mol^{-1}, with an LA yield of only 56.3% at 175 °C for 120 min using a composite catalytic system of Brønsted acid IL [IL-SO_3H]Cl and Lewis acid $NiSO_4$ (Table 1).[14] Garces et al. reported the conversion of HMF to LA in the Brønsted−Lewis acid β-zeolite catalyst with Brønsted acid HCl as a cocatalyst, and the highest LA yield was 61.7% at 140 °C (Table 1).[20]

Therefore, our results show great potential for using the dual-function $HScCl_4$ catalyst for the conversion of HMF to LA. In addition to the advantages of a high yield and low activation energy, the dual-function $HScCl_4$ catalyst biphasic system also makes it possible to carry out the reaction under mild conditions, that is, 120 °C for 35 min.

3. CONCLUSIONS

A novel dual-function Brønsted−Lewis acid $HScCl_4$ catalyst was developed for the catalytic conversion of HMF to LA. The results revealed that the $HScCl_4$ catalyst has excellent catalytic performance for reactions in a water−MIBK biphasic system. The synergistic catalytic effect of the Brønsted and Lewis acid sites of the $HScCl_4$ catalyst obviously decreases the energy barriers of the overall reaction, thus lowering the activation energy (E_a) and free energy (ΔG) of the reaction to 13.7 kJ mol^{-1} and −30 kcal mol^{-1}, respectively. Furthermore, the water−MIBK biphasic system, enhanced by the $HScCl_4$ salt effect, leads to efficient extraction of LA to the MIBK organic phase, thus minimizing the side reactions of LA and significantly improving the LA yield. The conversion of HMF and the selectivity for LA reach 100 and 95.6% at 120 °C after 35 min, respectively. The developed process provides a green sustainable and efficient pathway to produce platform chemicals of LA from biomass-derived HMF under mild conditions.

4. EXPERIMENTAL SECTION

4.1. Materials. HMF, LA, scandium chloride, MIBK, and other chemicals (analytical purity) were obtained from Sinopharm Chemical Reagent Co., Ltd. All materials were used without further purification unless otherwise explicitly stated.

4.2. Computational Method. All quantum calculations were performed with Gaussian software (Gaussian 09W Ver. 05, Gaussian, Inc.). The DFT method was adopted, and the standard 3-21G (*) basis set was used for all atoms. The geometries of catalysts and reactants were fully optimized using Berny's analytical gradient method,[40] and geometry optimiza-

https://doi.org/10.1021/acsomega.1c01607
ACS Omega 2021, 6, 15940−15947

tions were performed without symmetry restraints unless mentioned otherwise. In addition, vibrational frequency analysis based on the optimized structure was performed to decide whether the geometry of the reactant, molecular complexes, or products was a minimum on the potential energy surface or a transition state. The optimized geometries of the transition states were also characterized by one imaginary frequency, which was associated with a single eigenvalue of the Hessian matrix and confirmed by an IRC calculation method.[41]

4.3. Catalytic Reactions. The reaction was carried out in a 50 mL cylindrical stainless-steel reactor system (Dalian University of Technology Machinery Technology Co., Ltd., China) with external temperature and stirring controllers. In a typical procedure, HMF (1.0 g), $ScCl_3$ (0.27 mmol), 0.33 wt % HCl aqueous solution (3.0 g), and MIBK (10 mL) were loaded into the reactor. The reactor was sealed and purged with 0.3 MPa N_2 four times and then heated to the target temperatures for a preset duration with stirring at 400 rpm. After the reaction, the reactor was removed and rapidly cooled to 70 °C in a water bath, and then, the reaction mixture was stratified. The top layer was the mixture of products and analyzed by HPLC (LC-20AD), which was equipped with UV detection and an ODS-EP C_{18} reversed-phase column (250 mm × 4.6 mm, Intersil). The detection conditions were as follows: mobile phase, 15 mmol L^{-1} acetonitrile and phosphoric acid−sodium dihydrogen phosphate buffer solution (v_1/v_2 = 15:85); flow rate, 1.0 mL min^{-1}; column temperature, 30 °C. Formic acid was analyzed by HPLC equipped with an Aminex HPX-87H organic acid column and an RID-20A differential refractometer. The detection conditions were as follows: mobile phase, 5 mmol L^{-1} aqueous solution of sulfuric acid; flow rate, 0.55 mL min^{-1}; column temperature, 60 °C. The lower layer was a mixture of catalyst phases, including the catalyst, water, humins, and formic acid. When humins were filtered out and formic acid was removed by distillation, the catalyst was recovered. When a Lewis acid $ScCl_3$ catalyst was used, 2.0 g of H_2O was added to the reactor. When a Brønsted acid HCl catalyst was used, H_2O was not added. The conversion of HMF (X_{HMF}) and yields for LA (Y_{LA}), ALT (Y_{ALT}), and humins (Y_{Humins}) are defined in eqs 1−4. Here, $C_{HMF,0}$ and C_{HMF} are the initial and final concentrations of HMF, respectively, and C_{LA} and C_{ALT} are the final concentrations of LA and ALT, respectively. In addition, there are some products with a relatively low content, and we attribute the content of less than 0.2% to humins. During the reaction process, formic acid and LA were also formed. ALT was converted from LA; thus, the yield of formic acid was equal to the sum of the LA and ALT yields. By analyzing the HPLC data, it was found that the yield of formic acid was indeed the sum of the yields of LA and ALT. Therefore, the yield of formic acid is not listed in this article.

All definitions are on a molar basis.

$$X_{HMF} = \frac{(C_{HMF,0} - C_{HMF})}{C_{HMF,0}} \times 100\% \quad (1)$$

$$Y_{LA} = \frac{C_{LA}}{C_{HMF,0}} \times 100\% \quad (2)$$

$$Y_{ALT} = \frac{C_{ALT}}{C_{HMF,0}} \times 100\% \quad (3)$$

$$Y_{Humins} = 1 - Y_{LA} - Y_{ALT} \quad (4)$$

■ ASSOCIATED CONTENT

Supporting Information

The Supporting Information is available free of charge at https://pubs.acs.org/doi/10.1021/acsomega.1c01607.

DFT simulation calculation details, chemical structures of reactants and intermediates, FTIR spectra of the Brønsted−Lewis acidic catalyst using pyridine as a probe, kinetic analysis of the conversion of HMF to LA, cyclic test results, and thermogravimetric analysis results (PDF)

■ AUTHOR INFORMATION

Corresponding Authors

Yue Liu − *College of Chemical Engineering, Qingdao University of Science and Technology, Qingdao 266042, China*; Email: liuyue19890911@163.com; Fax: +86 532 84022719

Hailong Yu − *College of Chemical Engineering, Qingdao University of Science and Technology, Qingdao 266042, China; Limerick Pulp and Paper Centre, University of New Brunswick, Fredericton E3B5A3, Canada*; orcid.org/0000-0001-7712-2995; Email: yuhailong860220@163.com

Authors

Shiwei Liu − *College of Chemical Engineering, Qingdao University of Science and Technology, Qingdao 266042, China; Limerick Pulp and Paper Centre, University of New Brunswick, Fredericton E3B5A3, Canada*; orcid.org/0000-0002-0396-9883

Xueli Cheng − *College of Chemical Engineering, Qingdao University of Science and Technology, Qingdao 266042, China*

Shiqin Sun − *College of Chemical Engineering, Qingdao University of Science and Technology, Qingdao 266042, China*; orcid.org/0000-0001-8372-4001

Yige Chen − *College of Foreign Language, Qingdao University of Science and Technology, Qingdao 266042, China*

Bing Bian − *College of Chemical Engineering, Qingdao University of Science and Technology, Qingdao 266042, China; School of Chemical and Environmental Engineering, Shandong University of Science and Technology, Qingdao 266510, China*

Li Tong − *Limerick Pulp and Paper Centre, University of New Brunswick, Fredericton E3B5A3, Canada*

Yonghao Ni − *Limerick Pulp and Paper Centre, University of New Brunswick, Fredericton E3B5A3, Canada*; orcid.org/0000-0001-6107-6672

Shitao Yu − *College of Chemical Engineering, Qingdao University of Science and Technology, Qingdao 266042, China*

Complete contact information is available at: https://pubs.acs.org/10.1021/acsomega.1c01607

Notes

The authors declare no competing financial interest.

■ ACKNOWLEDGMENTS

We are grateful for financial support from the Shandong Provincial Natural Science Foundation Project

(ZR2019MC030), the open fund of the Key Laboratory of Biomass Energy and Materials of Jiangsu (JSBEM201802), the Key Research and Development Project of Shandong (2019GGX102021), the Natural Science Foundation of China (31370570), and the Taishan Scholars Projects of Shandong (ts201511033).

REFERENCES

(1) Zhang, J.; Liu, Y.; Yang, S.; Wei, J.; He, L.; Peng, L.; Tang, X.; Ni, Y. Highly selective conversion of furfural to furfural alcohol or levulinate ester in one pot over ZrO_2@SBA-15 and its kinetic behavior. *ACS Sustain. Chem. Eng.* **2020**, *8*, 5584−5594.
(2) An, L.; Si, C.; Wang, G.; Sui, W.; Tao, Z. Enhancing the solubility and antioxidant activity of high-molecular-weight lignin by moderate depolymerization via in situ ethanol/acid catalysis. *Ind. Crops Prod.* **2019**, *128*, 177−185.
(3) Han, Y.; Ye, L.; Gu, X.; Zhu, P.; Lu, X. Lignin-based solid acid catalyst for the conversion of cellulose to levulinic acid using γ-valerolactone as solvent. *Ind. Crops Prod.* **2019**, *127*, 88−93.
(4) Li, X.; Lu, X.; Nie, S.; Liang, M.; Yu, Z.; Duan, B.; Yang, J.; Xu, R.; Lu, L.; Si, C. Efficient catalytic production of biomass-derived levulinic acid over phosphotungstic acid in deep eutectic solvent. *Ind. Crops Prod.* **2020**, *145*, 112154.
(5) Chheda, J. N.; Huber, G. W.; Dumesic, J. A. Liquid-phase catalytic processing of biomass-derived oxygenated hydrocarbons to fuels and chemicals. *Angew. Chem., Int. Ed.* **2007**, *46*, 7164−7183.
(6) Šivec, R.; Grilc, M.; Huš, M.; Likozar, B. Multiscale modeling of (hemi)cellulose hydrolysis and cascade hydrotreatment of 5-hydroxymethylfurfural, furfural, and levulinic acid. *Ind. Eng. Chem. Res.* **2019**, *58*, 16018−16032.
(7) Sun, S.; Zhao, L.; Yang, J.; Wang, X.; Qin, X.; Qi, X.; Shen, F. Eco-friendly synthesis of SO_3H-containing solid acid via mechanochemistry for the conversion of carbohydrates to 5-hydroxymethylfurfural. *ACS Sustain. Chem. Eng.* **2020**, *8*, 7059−7067.
(8) Huang, X.; Kudo, S.; Sperry, J.; Hayashi, J.-i. Clean synthesis of 5-hydroxymethylfurfural and levulinic acid by aqueous phase conversion of levoglucosenone over solid acid catalysts. *ACS Sustain. Chem. Eng.* **2019**, *7*, 5892−5899.
(9) Yang, F.; Li, Y.; Zhang, Q.; Sun, X.; Fan, H.; Xu, N.; Li, G. Selective conversion of cotton cellulose to glucose and 5-hydroxymethyl furfural with SO_4^{2-}/M_xO_y solid superacid catalyst. *Carbohydr. Polym.* **2015**, *131*, 9−14.
(10) Jadhav, A. H.; Chinnappan, A.; Patil, R. H.; Kostjuk, S. V.; Kim, H. Green chemical conversion of fructose into 5-hydroxymethylfurfural (HMF) using unsymmetrical dicationic ionic liquids under mild reaction condition. *Chem. Eng. J.* **2014**, *243*, 92−98.
(11) Dutta, S.; Yu, I. K. M.; Tsang, D. C. W.; Su, Z.; Hu, C.; Wu, K. C. W.; Yip, A. C. K.; Ok, Y. S.; Poon, C. S. Influence of green solvent on levulinic acid production from lignocellulosic paper waste. *Bioresour. Technol.* **2020**, *298*, 122544.
(12) Tao, F.; Song, H.; Chou, L. Hydrolysis of cellulose in SO_3H-functionalized ionic liquids. *Bioresour. Technol.* **2011**, *102*, 9000−9006.
(13) Liu, S.; Wang, K.; Yu, H.; Li, B.; Yu, S. Catalytic preparation of levulinic acid from cellobiose via Brønsted-Lewis acidic ionic liquids functional catalysts. *Sci. Rep.* **2019**, *9*, 1810.
(14) Kumar, K.; Pathak, S.; Upadhyayula, S. 2nd generation biomass derived glucose conversion to 5-hydroxymethylfurfural and levulinic acid catalyzed by ionic liquid and transition metal sulfate: Elucidation of kinetics and mechanism. *J. Clean. Prod.* **2020**, *256*, 120292.
(15) Girisuta, B.; Janssen, L. P. B. M.; Heeres, H. J. A kinetic study on the decomposition of 5-hydroxymethylfurfural into levulinic acid. *Green Chem.* **2006**, *8*, 701−709.
(16) Asghari, F. S.; Yoshida, H. Kinetics of the decomposition of fructose catalyzed by hydrochloric acid in subcritical water: Formation of 5-hydroxymethylfurfural, levulinic, and formic acids. *Ind. Eng. Chem. Res.* **2007**, *46*, 7703−7710.
(17) Ramli, N. A. S.; Amin, N. A. S. Kinetic study of glucose conversion to levulinic acid over Fe/HY zeolite catalyst. *Chem. Eng. J.* **2016**, *283*, 150−159.
(18) Feng, J.; Tong, L.; Xu, Y.; Jiang, J.; Hse, C.; Yang, Z.; Pan, H. Synchronous conversion of lignocellulosic polysaccharides to levulinic acid with synergic bifunctional catalysts in a biphasic cosolvent system. *Ind. Crops Prod.* **2020**, *145*, 112084.
(19) Weiqi, W.; Shubin, W. Experimental and kinetic study of glucose conversion to levulinic acid catalyzed by synergy of Lewis and Brønsted acids. *Chem. Eng. J.* **2017**, *307*, 389−398.
(20) Garces, D.; Faba, L.; Díaz, E.; Ordóñez, S. Aqueous-phase transformation of glucose into hydroxymethylfurfural and levulinic acid by combining homogeneous and heterogeneous catalysis. *ChemSusChem* **2019**, *12*, 924−934.
(21) Xu, C.; Paone, E.; Rodríguez-Padrón, D.; Luque, R.; Mauriello, F. Recent catalytic routes for the preparation and the upgrading of biomass derived furfural and 5-hydroxymethylfurfural. *Chem. Soc. Rev.* **2020**, *49*, 4273−4306.
(22) Shi, X.; Nishiura, M.; Hou, Z. C−H polyaddition of dimethoxyarenes to unconjugated dienes by rare earth catalysts. *J. Am. Chem. Soc.* **2016**, *138*, 6147−6150.
(23) Gupta, N. N.; Punekar, A. S.; Raj, K. R.; Patil, V. S.; Gopinath, C. S.; Raja, T.; Raja, T. Phase transfer ceria-supported nanocatalyst for nitrile hydration reaction. *ACS Omega* **2019**, *4*, 16037−16044.
(24) Wang, C.; Luo, G.; Nishiura, M.; Song, G.; Yamamoto, A.; Luo, Y.; Hou, Z. Heteroatom-assisted olefin polymerization by rare-earth metal catalysts. *Sci. Adv.* **2017**, *3*, No. e1701011.
(25) Cotton, S. A. Scandium, yttrium & the lanthanides: Inorganic & coordination chemistry. *Encyclopedia of Inorganic Chemistry*, 2006.
(26) Shi, N.; Liu, Q.; Ju, R.; He, X.; Zhang, Y.; Tang, S.; Ma, L. Condensation of α-carbonyl aldehydes leads to the formation of solid humins during the hydrothermal degradation of carbohydrates. *ACS Omega* **2019**, *4*, 7330−7343.
(27) Velaga, B.; Parde, R. P.; Soni, J.; Peela, N. R. Synthesized hierarchical mordenite zeolites for the biomass conversion to levulinic acid and the mechanistic insights into humins formation. *Microporous Mesoporous Mater.* **2019**, *287*, 18−28.
(28) Li, X.; Xu, R.; Yang, J.; Nie, S.; Liu, D.; Liu, Y.; Si, C. Production of 5-hydroxymethylfurfural and levulinic acid from lignocellulosic biomass and catalytic upgradation. *Ind. Crops Prod.* **2019**, *130*, 184−197.
(29) Weingarten, R.; Kim, Y. T.; Tompsett, G. A.; Fernández, A.; Han, K. S.; Hagaman, E. W.; Conner, W. C.; Dumesic, J. A.; Huber, G. W. Conversion of glucose into levulinic acid with solid metal(IV) phosphate catalysts. *J. Catal.* **2013**, *304*, 123−134.
(30) Chambon, F.; Rataboul, F.; Pinel, C.; Cabiac, A.; Guillon, E.; Essayem, N. Cellulose hydrothermal conversion promoted by heterogeneous Brønsted and Lewis acids: Remarkable efficiency of solid Lewis acids to produce lactic acid. *Appl. Catal., B* **2011**, *105*, 171−181.
(31) Fukui, K. Role of frontier orbitals in chemical reactions. *Science* **1982**, *218*, 747−754.
(32) Cui, H.; Chen, D.; Zhang, Y.; Zhang, X. Dissolved gas analysis in transformer oil using Pd catalyst decorated $MoSe_2$ monolayer: A first-principles theory. *Sustainable Mater. Technol.* **2019**, *20*, No. e00094.
(33) Su, J. K.; Jin, Z.; Zhang, R.; Lu, G.; Liu, P.; Xia, Y. Tuning the reactivity of cyclopropenes from living ring-opening metathesis polymerization (ROMP) to single-addition and alternating ROMP. *Angew. Chem., Int. Ed.* **2019**, *58*, 17771−17776.
(34) Yang, G.; Pidko, E. A.; Hensen, E. J. M. Mechanism of Brønsted acid-catalyzed conversion of carbohydrates. *J. Catal.* **2012**, *295*, 122−132.
(35) Tang, Z.; Wang, W.; Pi, Y.; Wang, J.; Li, C.; Tan, R.; Yin, D. Visible-light-controlled reaction-separation for asymmetric sulfoxidation in water with photoresponsive metallomicelles. *ACS Sustain. Chem. Eng.* **2019**, *7*, 17967−17978.
(36) Zhang, C.; Song, Z.; Jin, C.; Nijhuis, J.; Zhou, T.; Noël, T.; Gröger, H.; Sundmacher, K.; van Hest, J.; Hessel, V. Screening of

https://doi.org/10.1021/acsomega.1c01607
ACS Omega 2021, 6, 15940−15947

functional solvent system for automatic aldehyde and ketone separation in aldol reaction: A combined COSMO-RS and experimental approach. *Chem. Eng. J.* **2020**, *385*, 123399.
(37) Ojha, D. K.; Kale, M. J.; McCormick, A. V.; Reese, M.; Malmali, M.; Dauenhauer, P.; Cussler, E. L. Integrated ammonia synthesis and separation. *ACS Sustain. Chem. Eng.* **2019**, *7*, 18785−18792.
(38) Patil, S. K. R.; Lund, C. R. F. Formation and growth of humins via aldol addition and condensation during acid-catalyzed conversion of 5-hydroxymethylfurfural. *Energy Fuels* **2011**, *25*, 4745−4755.
(39) Galletti, A. M. R.; Antonetti, C.; Ribechini, E.; Colombini, M. P.; Nassi o Di Nasso, N.; Bonari, E. From giant reed to levulinic acid and gamma-valerolactone: A high yield catalytic route to valeric biofuels. *Appl. Energy* **2013**, *102*, 157−162.
(40) Schlegel, H. B. Optimization of equilibrium geometries and transition structures. *J. Comput. Chem.* **1982**, *3*, 214−218.
(41) Safaei, Z.; Shayesteh, A. Ab initio calculations on sequential reactions of nitric oxide with titanium ions in the gas phase. *J. Phys. Chem. A* **2020**, *124*, 5194−5203.

https://doi.org/10.1021/acsomega.1c01607
ACS Omega 2021, 6, 15940−15947